Journal of Asian Earth Sciences 66 (2013) 204–214

Contents lists available at SciVerse ScienceDirect

Journal of Asian Earth Sciences

journal homepage: www.elsevier.com/locate/jseaes

V_P/V_S ratios in the upper crust of the southern Korean Peninsula and their correlations with seismic and geophysical properties

Eunyoung Jo, Tae-Kyung Hong *

Yonsei University, Department of Earth System Sciences, 50 Yonsei-ro, Seodaemun-gu, Seoul 120-749, South Korea

A R T I C L E I N F O

Article history:
Received 27 June 2012
Received in revised form 8 January 2013
Accepted 10 January 2013
Available online 26 January 2013

Keywords:
V_P/V_S ratio
Poisson's ratio
Upper crust
Korean Peninsula

A B S T R A C T

The *P* and *S* velocity ratio, V_P/V_S, is a seismic property that is convertible to Poisson's ratio, a widely-analyzed physical property of elastic materials. The lateral variation in the V_P/V_S ratios of the upper crust of the southern Korean Peninsula is investigated based on the travel times of *P* and *S* waves of local events with epicentral distances of 50 km or less and focal depths of 25 km or less. The dense seismic networks in the Korean Peninsula allow us to investigate the regional variation of V_P/V_S ratios. These V_P/V_S ratios are estimated to be 1.60–1.91 with an average of 1.69. The V_P/V_S ratios are as high as 1.73–1.91 in the Gyeongsang basin, Jeju island and offshore region of the eastern Okcheon belt, but have relatively low values of 1.64–1.72 in Precambrian massif regions. The stability of the V_P/V_S ratios is tested with randomly-resampled travel-time data, the results of which suggest nearly constant V_P/V_S ratios with increasing depth in the upper crust. The influences of plausible errors on origin times and arrival times are quantified to verify the V_P/V_S estimates. The V_P/V_S ratios are correlated with geological and tectonic structures. Comparisons with known seismic and geophysical properties suggest that structural features observed on the surface may extend at least to the mantle lid.

1. Introduction

Poisson's ratio is a diagnostic of medium compositions and properties such as lithology and rheology (Rudnick and Fountain, 1995; Christensen, 1996; Fernández-Viejo et al., 2005). Thus, Poisson's ratios have been widely analyzed in various studies to investigate the medium properties and compositions (Tatham, 1982; Musacchio et al., 1997; Mjelde et al., 2002; MacKenzie et al., 2008; Ji et al., 2009). The Poisson's ratios can be readily translated from the *P* and *S* velocity ratios, V_P/V_S (e.g., Salah and Seno, 2008), allowing for wide analysis of V_P/V_S ratios (e.g., Musacchio et al., 1997; MacKenzie et al., 2008).

Lateral variations of V_P/V_S ratios are typically well correlated with geological and tectonic structures. Thus, the V_P/V_S ratios have been widely used for investigation of tectonic structures, including active fault zones, forearcs, and volcanoes (e.g., Ojeda and Havskov, 2001; Chiarabba and Amato, 2003; Eberhart-Phillips et al., 2005; Moretti et al., 2009). The V_P/V_S ratios are also useful in studying the presence of partial melts and overpressured fluids in media (e.g., Julian et al., 1996; Nakajima et al., 2001; Salah and Seno, 2008). The partial melts and overpressured fluids can be identified by low *P* and *S* velocities and high V_P/V_S ratios (Sandvol et al., 1998; Zhao et al., 2002; Lin et al., 2007; Salah and Seno, 2008). On the other hand, the dehydrated serpentine regions of subducting plates are imaged by high seismic velocities and low V_P/V_S anomalies (e.g., Zhang et al., 2004; Reyners et al., 2006). Recently, the V_P/V_S ratios were interpreted along with other seismic and geophysical quantities for better estimation of water content of media (e.g., Eberhart-Phillips et al., 2005; Tondi et al., 2009).

The V_P/V_S ratios can be estimated by various approaches. One way is to use two independent *P* and *S* velocity models for calculation of V_P/V_S ratios (e.g., Nakajima et al., 2001). However, such analysis naturally incorporates unaccountable errors that are associated with manipulation of independent models based on the waves of different wavelengths. Another way is to calculate the V_P/V_S ratios directly from *P* and *S* travel times using a tomographic inversion, which requires a dense ray path coverage (Thurber and Atre, 1993; Wu et al., 2007). Such approach is, however, difficult to be achieved in low seismicity regions. Teleseismic receiver function analysis can also be used for estimating V_P/V_S ratios, which are, however, inherently limited by spatial distribution of seismic stations (e.g., Zhu and Kanamori, 2000; Chang and Baag, 2007). In addition, only the average V_P/V_S ratios of the medium above a certain internal boundary (e.g., Moho) can be estimated.

For a better interpretation of V_P/V_S ratios, it may be desirable to use methods that allow us to constrain the depth of imaging and to image fine lateral variation. The Wadati diagram was originally introduced to estimate the origin times of events (Wadati, 1933). The slope of the travel time data on a Wadati diagram can be

* Corresponding author. Tel.: +82 2 2123 2667.
E-mail addresses: jjoeun@yonsei.ac.kr (E. Jo), tkhong@yonsei.ac.kr (T.-K. Hong).

1367-9120/$ - see front matter © 2013 Elsevier Ltd. All rights reserved.
http://dx.doi.org/10.1016/j.jseaes.2013.01.008

expressed as a function of the V_P/V_S ratio in the medium. The Wadati analysis is based on P and S arrival time differences as a function of P arrival times. The Wadati analysis has been applied in studies of the medium properties of upper crusts and geothermal and volcanic regions (Griggs et al., 1975; Fitch and Rynn, 1976; Nicholson and Simpson, 1985; Chatterjee et al., 1985; Jiménez and García-Fernández, 1996).

The Wadati method can utilize seismic records for local seismic events, and does not require information on detailed crustal structures. Thus, the Wadati method is useful for regions with dense regional seismic networks. In this study, we use a modified Wadati method based on the travel times of local seismic waves from multiple events for the estimation of the V_P/V_S ratios in the upper crust of the southern Korean Peninsula. The variations in the V_P/V_S ratios with respect to geological and tectonic structures are examined. We investigate correlations with other seismic and geophysical quantities, and interpret the correlations in terms of the properties of the crust.

2. Tectonic and geological setting

The Korean Peninsula, located in the eastern margin of the Eurasian plate, experienced multiple and complex tectonic events, including continental rifting and collisions (e.g., Chough et al., 2000; Fig. 1). The landmass of the Korean Peninsula was most likely formed by collisions between the North and South China blocks during the Paleozoic to Jurassic (e.g., Chough et al., 2006; Oh, 2006; Hong and Choi, 2012). The East Sea (Sea of Japan) was opened by a backarc rifting during the Oligocene to mid-Miocene which separated the Japanese islands from the eastern Eurasian plate margin.

The Korean Peninsula shows features of a pure continental crust with a distinct internal boundary between the upper and lower crusts (He and Hong, 2010). The pure continental crust abruptly changes to a transitional crust across the east coast of the peninsula (e.g., Hong et al., 2008). The transitional crust was developed by the East Sea opening. The paleo-continental rifting developed a series of normal faults in regions off the east coast of the peninsula. The paleo-normal faults in the East Sea are reactivated to have thrustal motions by the compressional stress induced from the nearby plate boundaries with the Pacific and Philippine Sea plates (Choi et al., 2012).

The Korean Peninsula is primarily composed of three Precambrian massifs (Nangrim, Gyeonggi, and Yeongnam) and two intervening fold-thrust belts (Imjingang and Okcheon). The Okcheon belt is composed of the Taebaeksan basin in the east and the Okcheon metamorphic belt in the west (Chough et al., 2000; Cho and Kim, 2005). On the top of the Yeongnam massif, a Cretaceous volcanic-sedimentary basin (Gyeongsang) and a Tertiary sedimentary basin (Yeonil) have developed in the southeastern Korean Peninsula (Fig. 1). The volcanic sediments in the Gyeongsang basin are laid over the Yeongnam massif with a thickness of ~9 km or less (e.g., Choi, 1986; Cho et al., 2006). Jeju island is a volcanic island that was formed by multiple volcanic activities during the Pliocene epoch (end of the Tertiary) to Pleistocene epoch (early Quaternary).

Granites formed during the Triassic to middle Jurassic are distributed over the Gyeonggi and Yeongnam massifs and the northern boundary of the Okcheon belt (Sagong et al., 2005). Younger granites formed during the late Cretaceous to early Tertiary are found locally in the southern boundary of the Okcheon belt and the eastern Gyeongsang basin (Cho and Kim, 2005; Sagong et al., 2005). Metamorphic rocks are abundantly distributed in the western Okcheon belt. In addition, ultramafic rocks occur locally in the northern Gyeongsang basin (Whattam et al., 2011).

3. Seismic and geophysical properties

Various geophysical and seismic quantities of the crust of the southern Korean Peninsula are presented in Fig. 2 with geological provinces defined by the surface geology. The presented geophysical and seismic quantities are heat flows on the surface (Lee et al., 2010; Fig. 2a), Moho P velocities (Hong and Kang, 2009; Fig. 2b),

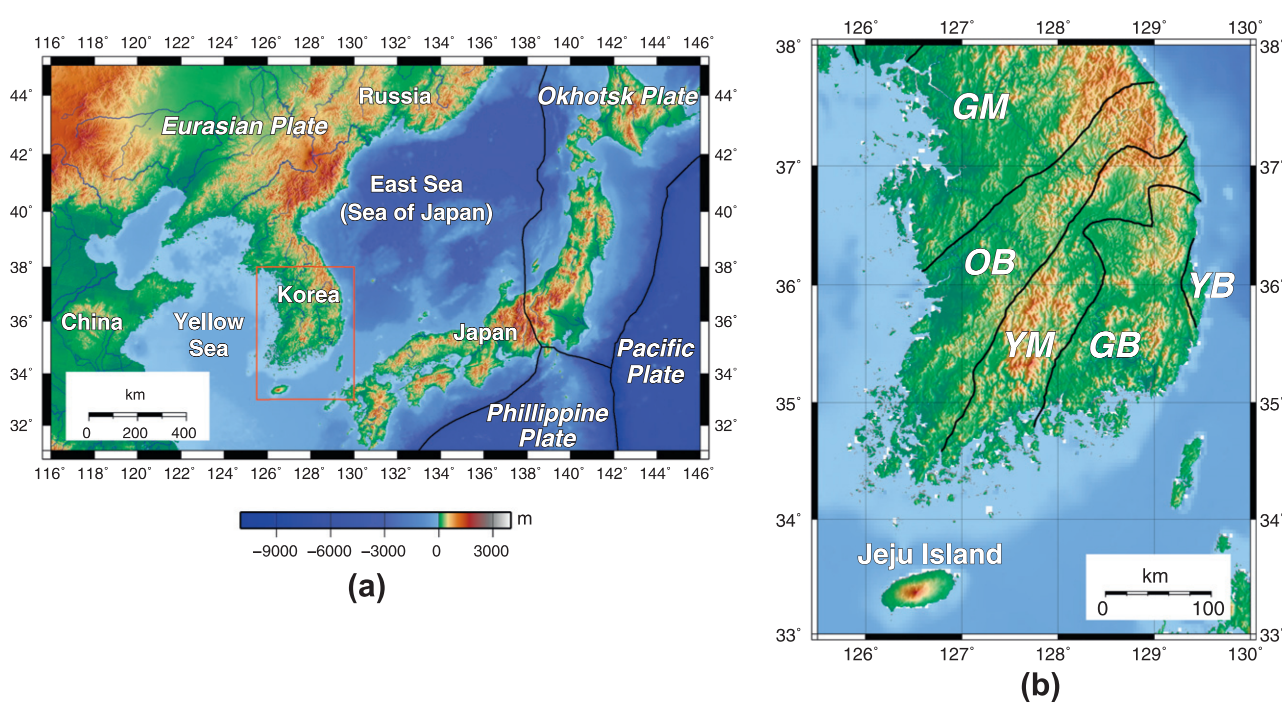

Fig. 1. Map of geological and tectonic structures: (a) major tectonic structures around the Korean Peninsula and (b) an enlarged map of the study region with annotation of geological structures. The Korean Peninsula is located in the eastern margin of the Eurasian plate. Major geological structures on the map include the Gyeongsang basin (GB), Gyeonggi massif (GM), Okcheon belt (OB), Yeonil basin (YB), and Yeongnam massif (YM).

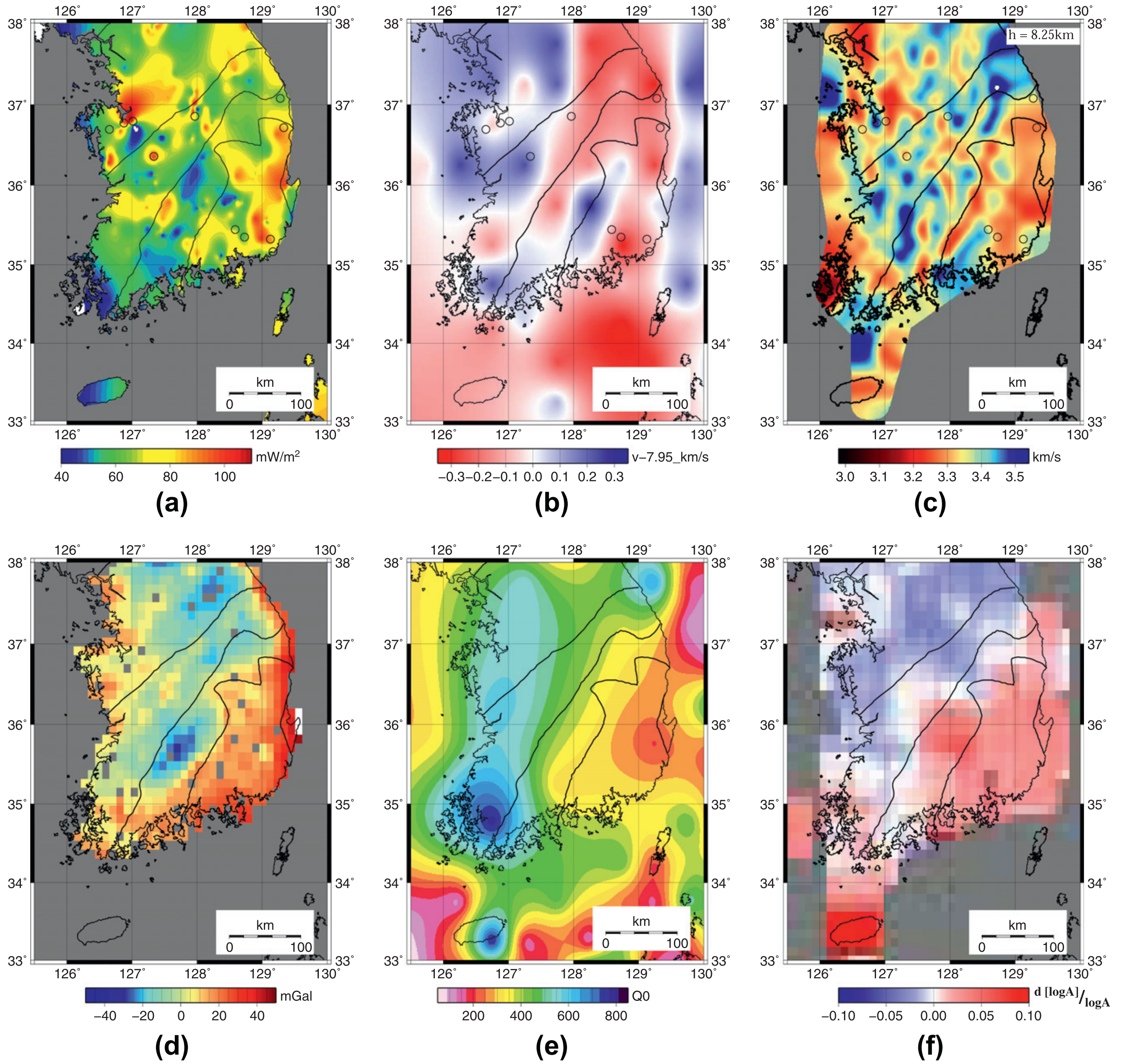

Fig. 2. Seismic and geophysical estimates of the study region: (a) Heat flows, (b) Moho *P* (*Pn*) velocities, (c) shear-wave velocities at a depth of 8.25 km, (d) Bouguer gravity anomalies, (e) crustally-guided shear wave attenuation factor (Lg Q_0), and (f) crustal *P* amplification factor. The locations of major hot springs are indicated by open circles on the maps of heat flows, Moho *P* velocities and upper-crustal *S* velocities. High correlations with positive or negative proportions are observed among the various estimates.

upper-crustal shear-wave velocities (Choi et al., 2009; Fig. 2c), Bouguer anomalies (Cho et al., 1997; Fig. 2d), crustally-guided shear-wave (*Lg*) attenuation factor (Hong, 2010; Fig. 2e), and crustal *P* amplification factor (Hong and Lee, 2012; Fig. 2f).

The average heat flow on the Earth's surface is observed to be about 70 mW/m^2 in the southern Korean Peninsula (Lee et al., 2010). However, relatively high heat flows of about 85 mW/m^2 or greater are observed on the surfaces of the Gyeongsang basin, the west-central Gyeonggi massif, and the eastern Okcheon belt. Relatively low heat flows of about 45 mW/m^2 or lower are reported in the southern Yeongnam massif, the western end of Okcheon belt, and at Jeju island (Lee et al., 2010).

The average *P*-wave velocity on the Moho is 7.95 km/s, which is lower than the global average of the continental crust, which is 8.05 km/s (Hong and Kang, 2009). Relatively high Moho *P*-wave velocities are observed in the Gyeonggi massif, western ends of Okcheon belt and Yeongnam massif, and central Yeongnam massif. On the other hand, low Moho *P* velocities are observed in the eastern Okcheon belt, the eastern Yeongnam massif, and Gyeongsang basin. A north–south directional high velocity anomaly is observed in the region off the east coast of the peninsula. It is noteworthy that the Moho *P* velocities are highly anti-correlated with the heat flows.

The *S*-wave velocities at a depth of 8.25 km were calculated by Choi et al. (2009) using ambient noises recorded at local and regional stations. Rayleigh waves traveling between pairs of stations can be extracted by the cross-correlation of ambient noise records between stations (e.g., Shapiro et al., 2005). The use of high-frequency seismic energy with short inter-station distances presents a small-scale variation in *S* velocities. The Gyeongsang basin, western Gyeonggi massif, and Okcheon belt present relatively low *S* velocities of ∼3.2 km/s or lower, while most other regions show *S* velocities of 3.4 km/s or greater.

The Bouguer gravity anomaly appears to be correlated with the surface topography. Negative Bouguer anomalies of about −15 mGal are observed in the eastern Gyeonggi massif, eastern Okcheon belt, and central Yeonggnam massif. On the other hand, positive gravity anomalies of 20–40 mGal are apparent around Gyeongsang basin (Cho et al., 1997). The *Lg* waves and *P* waves display similar features of attenuation and amplification. Low *Lg* attenuations and low *P* amplification are present in the Gyeonggi massif and Okcheon belt (Hong, 2010; Hong and Lee, 2012). However, high *Lg* attenuation and high *P* amplification are observed in the Gyeongsang basin. Jeju island shows low *Lg* attenuation and high *P* amplification.

4. Data

Seismic waveforms of local events during 1999–2011 are collected from seismic networks in the southern Korean Peninsula (Fig. 3a). The event information is collected from the Korea Meteorological Administration (KMA) and the Korea Institute of Geosciences and Mineral Resources (KIGAM) that operate dense seismic networks in the southern Korean Peninsula. The total number of events is 359, most of which occurred in the upper crust at depths of 20 km or less. (Fig. 3b). The number of stations used in this study is 122.

To avoid interference by other crustal phases, we delimit the seismic records with epicentral distances of 50 km or less in which direct *P* and *S* waves are the first-arrival phases (Fig. 3c). The arrival times of the direct *P* and *S* waves (*Pg*, *Sg*) are determined manually by careful examination of three-component local seismic records. The total number of *P* and *S* travel-time pairs is 1122.

5. Method

The Wadati analysis was originally introduced to determine the origin times of events from the arrival times of *P* and *S* waves (Wadati, 1933). The Wadati analysis is based on a diagram presenting the arrival time differences between *P* and *S* waves as a function of *P* arrival times. The arrival time data are fitted by a least-squares line. The origin time of an event is the time at which the least-square line crosses the *P*-arrival-time axis.

The slope of the least-squares line is given by (e.g., Yoshiyama, 1957)

$$\mathrm{Slope} = \frac{T_S - T_P}{T_P} = \frac{V_P}{V_S} - 1, \tag{1}$$

where T_P and T_S are the travel times of the *P* and *S* waves. The slope of the least-squares line can be expressed in terms of the V_P/V_S ratio. The Poisson's ratio, ν, can be expressed as a function of the V_P/V_S ratio (e.g., Carpenter and Cash, 1988):

$$\nu = \frac{1}{2}\left[1 - \frac{1}{(V_P/V_S)^2 - 1}\right]. \tag{2}$$

An example of Wadati analysis for the 20 January 2007 M_L4.8 earthquake using the arrival times of direct phases (*Pg*, *Sg*) is presented in Fig. 4. The focal depth of the event is 13.1 km. The seismic data are collected from stations with epicentral distances of 100 km or less. The number of arrival-time data is 17. The origin time is determined to be 11:56:53.57 (UTC), which is very close to the reported origin time of 11:56:53.6 (UTC). The V_P/V_S ratio is determined to be 1.713. The standard deviation of arrival-time data with respect to the least-squares line is 0.280 s.

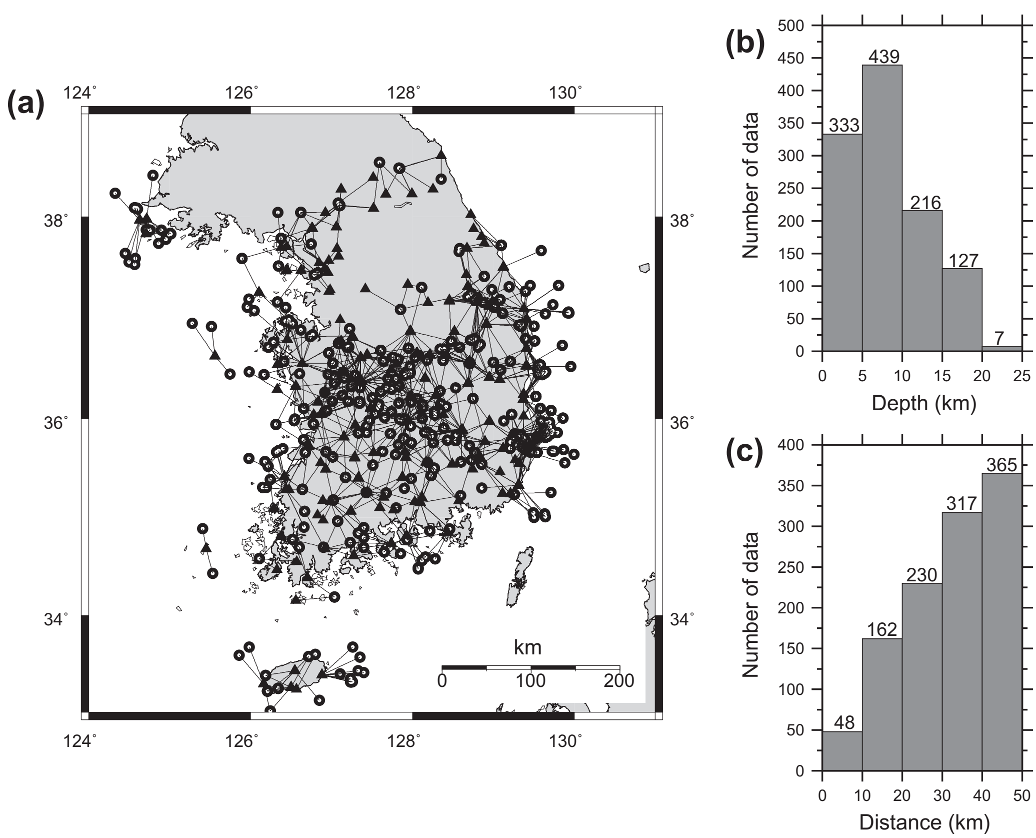

Fig. 3. (a) Map of events (circles) and stations (triangles) analyzed in this study. The great-circle paths between the events and stations are marked with solid lines. (b) Histogram of data points with focal depths. (c) Histogram of data points with distances. The numbers of events and stations are 359 and 122. The total number of pairs is 1122. Most events are clustered at depths less than 20 km. The distances are less than 50 km.

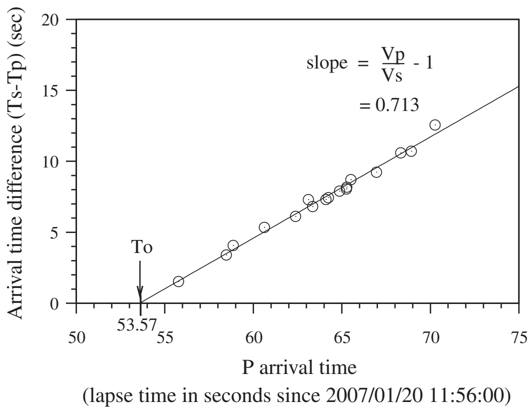

Fig. 4. An example of determining the origin time of the 20 January 2007 M4.8 earthquake from travel time differences between *P* and *S* waves as a function of *P* arrival times using a Wadati diagram. The number of data points is 17. The travel time data are fitted with a least-squares line. The standard deviation of the data from the least-squares line is 0.280 s. The intercept of line on the horizontal axis, T_0, indicates the origin time of event, which is 11:56:53.57. The slope of the line indicates the average V_P/V_S, which is 1.713.

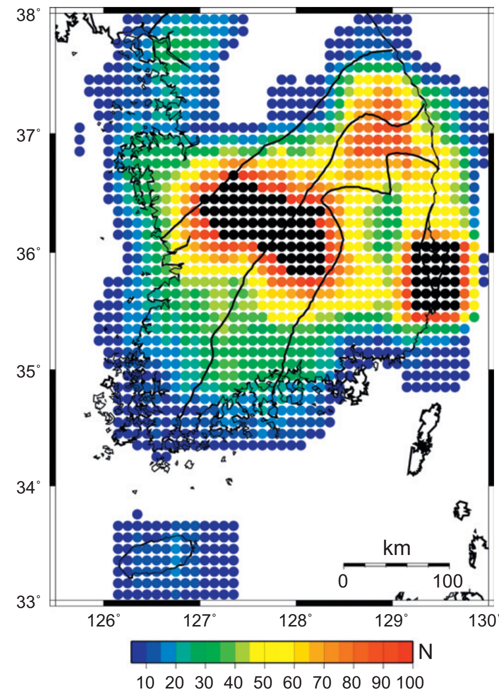

Fig. 6. The numbers of data points in discrete cells dividing the study region. The numbers of data points vary between 5 and 133. The numbers of data points are larger than 10 in most cells. The densities of data are high in the Okcheon belt and eastern Gyeongsang and Yeonil basins, but are relatively low in the northern region around the eastern Gyeonggi massif.

In this study, we modify the original Wadati method by assembling multiple events in order to improve the stability in determining the V_P/V_S ratios of media. We analyze the travel times of seismic waves instead of the arrival times in order to assemble data from multiple events with different origin times. To improve the determination of representative V_P/V_S ratios of local regions, the data are classified by region based on the locations of events and stations. It is noteworthy that this method dose not require focal-depth information, which typically has larger errors than the epicenters. This feature allows us to estimate the representative V_P/V_S ratios in the medium without high-precision focal-depth information.

The study region is discretized by uniform-sized cells that are sufficiently large to include each event-station pair. Additionally, the cell size should be small enough so that the medium in each cell can be assumed to be uniform. We discretize the southern Korean Peninsula into 0.7°-by-0.7° cells. Each cell overlaps with neighboring cells by 0.6° in longitude and latitude. The representative V_P/V_S ratio of each cell is estimated at every 0.1° in longitude and latitude.

Considering possible errors in collected source parameters, travel time data deviating from the least-squares lines by 1.0 s or greater are excluded in the modified Wadati analysis in order to enhance the stability of results (Fig. 5). Also, only the cells with five or more data points are analyzed to ensure stable measurement of V_P/V_S ratios (Fig. 6). There are as many as 133 data points in the central and southeastern regions. The data coverage is relatively poor in the northern region. However, most regions have more than 10 data points.

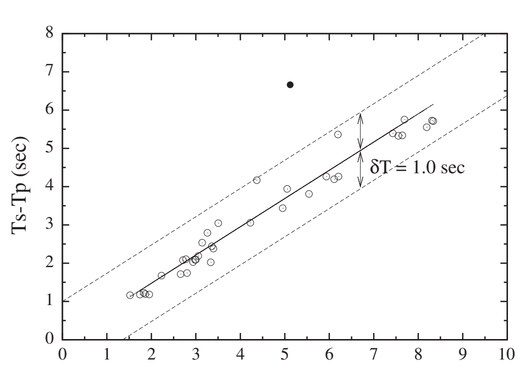

Fig. 5. An example of an analysis based on a modified Wadati diagram to determine a representative V_P/V_S ratio from travel time data of local events. Travel time data with deviations (δT) from the least-squares line by 1.0 s or greater (closed circle) are removed from the analysis.

The V_P/V_S ratios can be estimated from the T_S/T_P ratios (e.g., Chatterjee et al., 1985; Jiménez and García-Fernández, 1996). In this study, the V_P/V_S ratios are estimated from $(T_S - T_P)/T_P$ ratios, as shown in Eq. (1). The large deviations in the travel-time data from the least-squares lines suggest the presence of large errors either in the phase arrival times or event origin times. It is known that phase-picking errors typically generate random errors, while origin time errors cause systematic shifts in travel times. Thus, the observed features of travel-time data may allow us to identify the source of errors. It is noteworthy that the travel times of seismic waves are dependent not only on the epicentral distances, but also on the focal depths. As the Wadati analysis does not require the focal-depth information, the estimated V_P/V_S ratios are hardly dependent on the focal depths of events.

6. V_P/V_S ratios

The V_P/V_S ratios in the upper crust of the southern Korean Peninsula are estimated to be in the range of 1.60–1.91 (Fig. 7a). The average V_P/V_S ratio is 1.69. The equivalent Poisson's ratios are 0.18–0.32, with an average of 0.23 (Fig. 7b). It is known that the Poisson's ratios of crustal rocks mostly vary between 0.2 and 0.3 (e.g., Lillie, 1998). It is noteworthy that that the estimated average V_P/V_S ratio is lower than that of the Poisson solid (=1.73) which has been assumed for the crust of the Korean Peninsula (e.g., Chang and Baag, 2005).

The V_P/V_S ratios are observed to be high in the Yeonil and eastern Gyeongsang basins (region A in Fig. 7a), the coastal region off

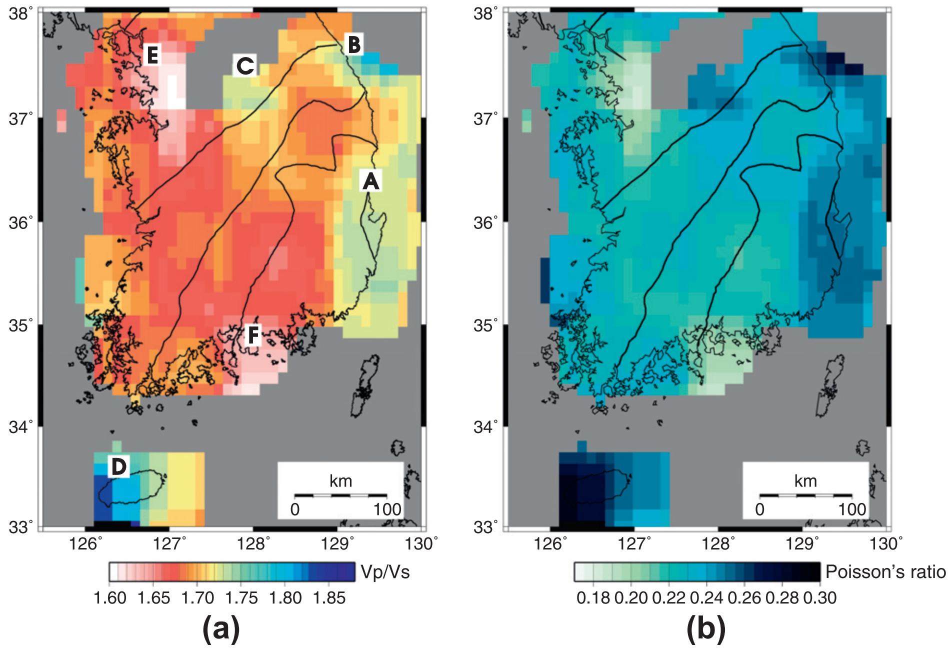

Fig. 7. (a) The resultant V_P/V_S ratios and (b) the equivalent Poisson's ratios. The V_P/V_S ratios vary between 1.60 and 1.91, and the Poisson's ratios vary between 0.18 and 0.32. High V_P/V_S ratios are observed in regions A, B, C and D, while low V_P/V_S ratios are found in regions E and F.

the eastern Okcheon belt (region B), the south-central Gyeonggi massif (region C), and the western Jeju island (region D). The V_P/V_S ratios in the eastern Gyeongsang basin are as high as 1.73–1.76, and those in western Jeju island are 1.76–1.91. However, relatively low V_P/V_S values are observed in other regions, which are as low as 1.60–1.72 and with an average of 1.68. In particular, low V_P/V_S anomalies prevail in the western Gyeonggi massif (region E) and southwestern margin of the Gyeongsang basin (region F).

The V_P/V_S ratios vary with the mineral and rock compositions in the medium. Thus, the estimated V_P/V_S ratios reflect the properties of the upper crust (Fernández-Viejo et al., 2005). Low and high V_P/V_S ratios suggest the dominance of felsic and mafic rocks in the medium, respectively (Christensen, 1996; Ji et al., 2009). The V_P/V_S ratios are relatively high in the eastern Gyeongsang basin and Jeju island where volcanic or volcaniclastic rocks are prevalent. On the other hand, relatively low V_P/V_S ratios are apparent in most regions of Gyeonggi and Yeonggnam massifs.

7. Stability and verification tests

The validity of the results is tested by examining the influences of error-inducing factors in the V_P/V_S analysis. We first examine the stability of the results using a bootstrap method (e.g., Efron and Tibshirani, 1991; Revenaugh and Meyer, 1997; Hong and Menke, 2008). The variability of the V_P/V_S ratios with focal depth is examined by the stability test. The travel time data are randomly resampled from the original data set of each cell with allowance for duplicate selections. We construct 100 resampled data sets using the bootstrapping. The V_P/V_S ratios are determined for every resampled data set. The average V_P/V_S ratios and standard deviations among the V_P/V_S estimates for the 100 resampled data sets are presented in Fig. 8.

The standard deviations are less than 0.01 in most inland regions, but are slightly higher around the coastal regions (up to 0.02). Western Jeju island shows relatively low consistency in V_P/V_S ratios among the resampled data sets. This feature may be associated with the number of data points available in the region, which is too small to make a stable determination. A similar feature is observed in the deviations of the V_P/V_S ratios for the data set with respect to the reference V_P/V_S ratios. The overall observations show that the V_P/V_S ratios are consistent among resampled data sets in most regions, suggesting the stability of the results. This observation suggests that the V_P/V_S ratios may be nearly constant with increasing depth in the upper crust.

We next quantify the effects of possible errors in the determination of V_P/V_S ratios. The errors in the travel time data may be due to inaccurate origin times and phase picking. In addition, inhomogeneities in media can cause perturbation in travel times. Errors in origin times cause constant shifts in the travel times of both *P* and *S* waves (T_P, T_S). On the other hand, phase-picking errors may cause random travel-time errors independent from the seismic phase. Also, inhomogeneous media may cause raypath-dependent variations in travel times. In this study, we analyze seismic data with distances of less than 50 km, over which the media along ray paths can be approximated to be homogeneous. Thus, the errors induced by the inhomogeneities in media should be insignificant.

Origin time errors may not exceed a few tenths of a second when considering the seismic velocities in the upper crusts and the epicentral distances. Similarly, event-location errors may not be greater than 3 km when considering epicentral distances and crustal velocities. Event-location errors are equivalent to origin-time errors of ~0.5 s or less. These origin-time errors cause constant travel-time shifts in the Wadati diagram. The travel-time data with noticeable differences from remanent data can be removed from the analysis.

The possible V_P/V_S variation by the origin-time errors is examined. The origin-time errors are represented by random errors with a Gaussian distribution between −0.5 s and 0.5 s. The same size of error is applied to travel time data from a common event. The sizes of errors are different for each event. The deviations of the V_P/V_S ratios caused by origin-time errors are less than 0.04 in most regions, with deviations greater than 0.1 occurring in the region off the west coast of Jeju island (Fig. 9).

Considering the typical waveforms of moderate-sized earthquakes in local distances, the phase picking errors may not exceed

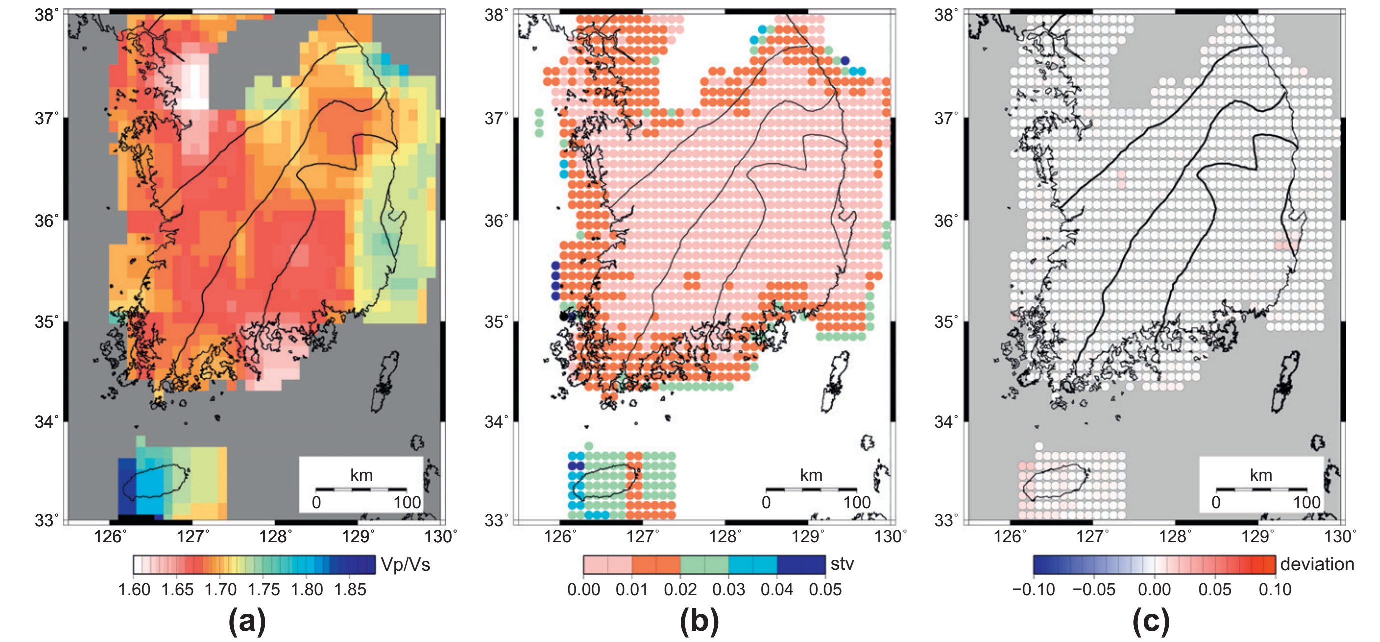

Fig. 8. Stability test of V_P/V_S ratios based on 100 randomly selected data sets: (a) average V_P/V_S ratios of 100 random data sets, (b) standard deviations, and (c) deviations between the reference V_P/V_S ratios and estimates from a randomly-selected data set. The standard deviations among the V_P/V_S ratios are less than 0.02 in most regions. The magnitudes of the deviations between the reference V_P/V_S ratios and the estimates from a random data set are far less than 0.005 in most regions. The observations suggest that the estimates of V_P/V_S ratios are consistent among the random sets.

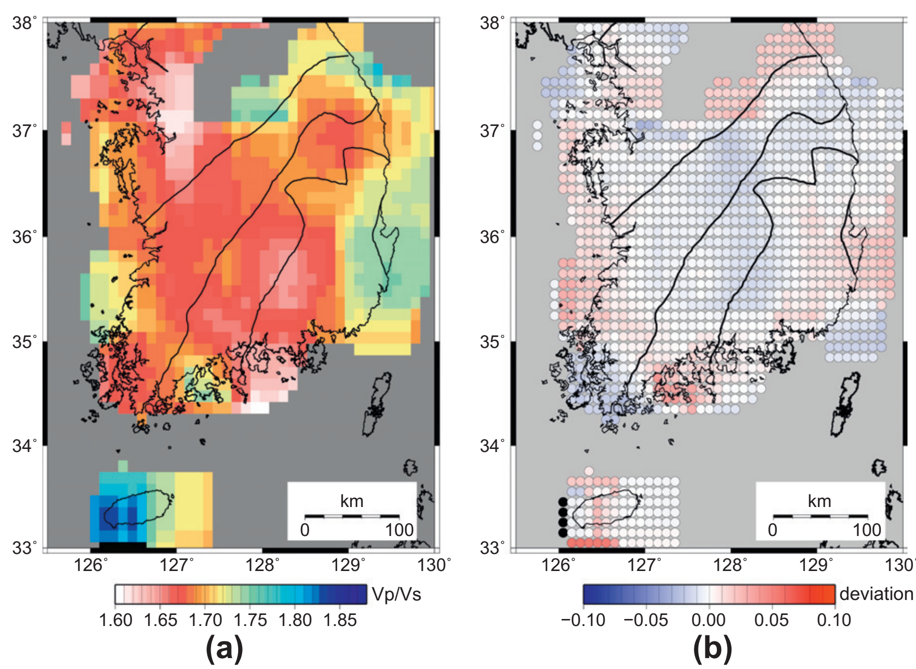

Fig. 9. (a) Examination of V_P/V_S ratios with addition of Gaussian random errors to origin times and their deviations from the reference V_P/V_S ratios. The random errors are designed to be between −0.5 s and 0.5 s. The magnitudes of the deviations are less than 0.04 in most regions.

±0.1 s for *P* waves and ±0.2 s for *S* waves (Fig. 10). The phase picking errors may be dependent on the waveforms, picking algorithms, and other unaccountable factors. Thus, phase picking errors may be presented as random errors.

The effects of phase picking errors on V_P/V_S estimates are examined by contaminating the travel times with random errors with homogeneous distribution between −0.1 and 0.1 s for *P* waves, and between −0.2 and 0.2 s for *S* waves. The deviations in the V_P/V_S ratios are less than 0.01 in most regions, with the highest deviations of around 0.03 in regions off the east coast of Jeju island (Fig. 11). This observation suggests that plausible errors in phase picking may not induce significant variation in V_P/V_S estimates. Overall, the validity and stability tests of V_P/V_S ratios present that the V_P/V_S estimates are stable, even with contamination with various sources of errors on travel times, confirming the validity of the results.

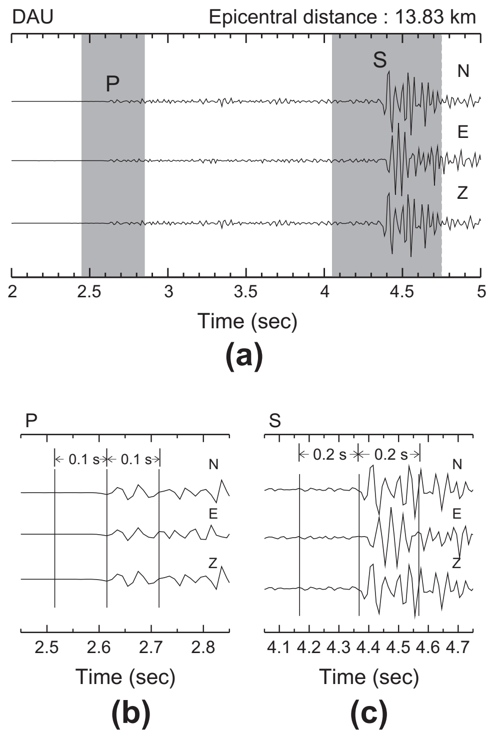

Fig. 10. (a) Example of a three-component local seismogram from station DAU for the 2 April 2011 M_L2.5 earthquake, which had a focal depth of 4.9 km, and enlarged waveforms around the (b) *P* and (c) *S* phases. The epicentral distance is 13.83 km. The *P* and *S* arrival times are indicated by solid lines in the enlarged waveforms, and plausible error ranges in phase picking are marked with dotted lines. The plausible error ranges are −0.1 to 0.1 s for *P* waves, and −0.2 to 0.2 s for *S* waves.

8. Correlations with seismic and geophysical properties

The V_P/V_S ratios are compared with six different geophysical and seismic properties (Fig. 2). The seismic and geophysical properties are dependent on petrological composition, rheology, density, water content and temperature of the medium. The manner of correlation between various geophysical and seismic properties allows us to infer the properties of the crust in the southern Korean Peninsula.

The heat flow on the Earth's surface is a combined effect of heat from the crust, lithospheric mantle, and Earth's deep interior (e.g., Jaupart and Mareschal, 2007). In the continental lithospheres, the crust and lithospheric mantle affect the heat flows on the Earth's surface not only by the presence of heat sources, but also by the thermal conductivity, which is dependent on the medium composition. Active tectonics such as continental rifting or arc collisions are absent in the Korean Peninsula. Also, considering the area of the southern Korean Peninsula, the heat flows originating from the Earth's deep interiors should be nearly uniform over the study region. Thus, the variation of the heat flows on the surface may be mainly controlled by the heat sources in the crust and lithospheric mantle.

A comparison between the heat flows and *Pn* velocities helps us infer the properties in the lithospheric mantle (e.g., Black and Braile, 1982). The *Pn* velocities are observed to be highly anti-correlated with V_P/V_S ratios in most regions except the western Gyeonggi massif, where high heat flows are present (region E). Also, the *Pn* velocities are generally anti-correlated with the surface heat flow and the upper-crustal *S* velocities (Fig. 2).

Low *Pn* velocities are observed in high heat flow regions such as the eastern Gyeongsang basin, Yeonil basin, eastern Okcheon belt, and western Gyeonggi massif, while high *Pn* velocities in low heat flow regions such as the northern Gyeonggi massif, western Okcheon belt, and southern Yeongnam massif. The V_P/V_S ratios appear to be highly correlated with the heat flows. Relatively low V_P/V_S ratios are observed in low heat flow regions, while relatively high V_P/V_S ratios are observed in high heat flow regions. On the other hand, the shear-wave velocities at a depth of 8.25 km appear to be anti-correlated with V_P/V_S ratios and heat flows in most regions, except the Gyeongsang basin region in which thick volcanic sediments cover the Yeongnam massif up to a depth of about 9 km.

It is known that the crustal medium of the Gyeonggi massif is composed primarily of Precambrian felsic granite, the V_P/V_S ratios of which are expected to be high (Christensen, 1996). However, the western Gyeonggi massif region (E in Fig. 7a) presents high heat flows, low *Pn* velocities, low upper-crustal *S* velocities, and low V_P/V_S ratios. It should be noted that the region is geographically identical to a hot spring region (the Onyang hot spring region). The low V_P/V_S ratios in the upper crust may be explained by medium perturbation due to high heat flows (e.g., increase of pore pressure) (Jiménez and García-Fernández, 1996; Julian et al., 1996).

For comparison, major hot spring regions are marked on the maps for heat flows, Moho *P* (*Pn*) velocities and upper crustal *S* velocities (Fig. 7a–c). The hot springs appear to be generally located in and around high or mildly high heat flow and low seismic velocity regions, with the exception of the Yuseong hot spring in the western Okcheon belt, which has high heat flows and low upper crustal *S* velocities, but high *Pn* velocities.

The similar low velocity anomalies in both the Moho and the upper crust suggest that high heat flows on the surface may primarily originate from the lithospheric mantle. However, the Yuseong hot spring is placed on a small high heat flow. The spatial dimension of the heat flow and the seismic velocities in the Moho and upper crust suggest that the heat source may be located in the upper crust, which is also supported by the relatively low upper-crustal V_P/V_S ratios.

High Bouguer gravity anomalies and high V_P/V_S ratios are present in the eastern Gyeongsang basin (region A in Fig. 7a) and off the eastern Okcheon belt (region B), where multiple volcanic activities and a paleo-rifting event occurred (Chough et al., 2000; Choi et al., 2012). The high Bouguer gravity anomalies suggest the presence of high density materials in the medium, which is consistent with observations of magma underplating and Tertiary basaltic rocks (e.g., Chough et al., 2000; Cho et al., 2004).

However, relatively low V_P/V_S ratios are apparent in the western Okcheon belt, western Yeongnam massif and western Gyeongsang basin in which heat flows are relatively low and *Pn* velocities are relatively high. These regions coincide approximately with the locations where old granite formed during the Triassic to Jurassic is observed on the surface (Sagong et al., 2005). On the other hand, relatively high V_P/V_S ratios and low *Pn* velocities are observed in the metamorphic regions between the Gyeonggi massif and Okcheon belt and the central boundary between the Yeongnam massif and Okcheon belt (Chough et al., 2000). In addition, the V_P/V_S ratios are estimated to be high in the ultramafic–mafic complex regions at the southwestern Gyeonggi massif (Baekdong, Bibong, Yugu) and northwestern Gyeongsang basin (Andong) (Whattam et al., 2011).

The Gyeongsang basin can be clearly identified by the crustal shear wave velocities, crustal *P* amplification, and *Lg* attenuation. The sedimentary layer structure of the Gyeongsang basin displays a characteristic low velocity structure. In addition, the sedimentary layer amplifies the near-vertically incident *P* waves, and attenuates the crustally-guided shear waves.

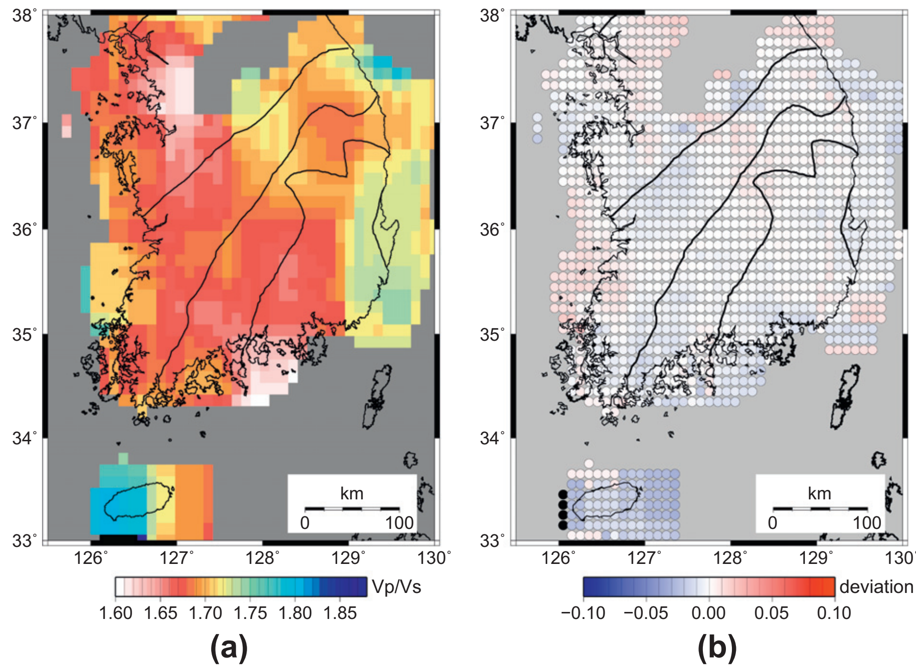

Fig. 11. (a) Examination of V_P/V_S ratios for the addition of random errors in phase picking and (b) their deviations from the reference V_P/V_S ratios. Random errors of −0.1 to 0.1 s are applied for *P* travel time data, and random errors of −0.2 to 0.2 s are applied for *S* travel time data. The deviations are close to zero in most regions, suggesting high stability and reliability of the results.

9. Discussion

Chang and Baag (2007) estimated the crustal V_P/V_S ratios to be 1.71–1.82 using a receiver function analysis based on teleseismic records from 21 broadband stations deployed in the southern Korean Peninsula. Those estimates are under the range of the V_P/V_S ratios estimated in this study. It should be noted that the V_P/V_S estimates of Chang and Baag (2007) represent the average crustal V_P/V_S ratios above the Moho, whereas the V_P/V_S ratios estimated in this study represent the properties of upper crust. The spatial resolution of the V_P/V_S estimates of Chang and Baag (2007) are relatively poor due to large spatial intervals between stations. On the other hand, this study is based on large numbers of stations and events, allowing us to resolve fine lateral variation in V_P/V_S ratios.

Chang and Baag (2007) reported relatively high V_P/V_S ratios in the Yeongnam massif and Gyeongsang basin, and relatively low V_P/V_S ratios in the Gyeonggi massif. The highest V_P/V_S ratio was observed in the eastern Gyeongsang basin, and the lowest V_P/V_S ratio in the eastern Gyeonggi massif. Localized low V_P/V_S ratios were found around the western Gyeonggi massif. There is some similarity between the V_P/V_S ratios reported by Chang and Baag, 2007 and those estimated in this study such as the location of the highest V_P/V_S ratio. Also, the existence of a localized low V_P/V_S ratio in the western Gyeonggi massif is consistent between the studies.

This study, however, found relatively high V_P/V_S ratios in the eastern Gyeonggi massif, which is not consistent with the observation of Chang and Baag (2007). In addition, the relatively low V_P/V_S ratios in the western border between the Yeongnam massif and Gyeongsang basin are not apparent in Chang and Baag (2007). Further, Chang and Baag (2007) reported considerable differences in the V_P/V_S ratios between the central Korean Peninsula (Gyeonggi massif) and the southern Korean Peninsula (Yeongnam massif and Gyeongsang basin), which however is hardly identifiable in this study. This feature may be associated with differences in the depths of imaging and the vertical geometry of the geological provinces.

There appears to be a general correlation in the lateral variations between Bouguer gravity anomalies, crustally-guided shear-wave attenuation (*Lg Q*), crustal *P* amplification, and upper-crustal *S*-wave velocities. In addition, a high correlation between *Pn* velocities and heat flows is observed. The correlations among the geophysical and seismic properties are due to the quasi-linear relationship between the perturbations of seismic velocities and densities, which has been well conceived in many studies (e.g., Birch, 1961; Sato and Fehler, 1998; Hong et al., 2004).

However, as the variations in the *P* and *S* velocities differ by medium, the velocity ratios (V_P/V_S) do not change linearly with the seismic velocities. Thus, the V_P/V_S ratios display a characteristic variation that displays local correlations with geophysical and seismic quantities. A composite analysis of V_P/V_S ratios with other geophysical and seismic quantities may help us to constrain the medium properties.

The examination of the correlation between the Moho *P* (*Pn*) velocities and upper-crustal *S* velocities allows us to infer the vertical extent of the anomalies and to identify the sources of the anomalies. Relatively strong anti-correlations are observed in the eastern Okcheon belt, Gyeonggi massif (except the western high heat flow region), and the southern Yeongnam massif. This observation suggests that the physical properties of a medium (e.g., the level of deformation) or the chemical properties of a medium (e.g., the dominant lithological composition) may differ between the upper and lower crusts.

Positive correlations are found in some local regions, including the western Okcheon belt, the southwestern Yeongnam massif, and the eastern Gyeongsang basin. This observation suggests that such positive-correlation regions may have experienced lithospheric deformation after the formation of the Korean Peninsula during the Paleozoic to Jurassic. The composite set of geophysical and seismic properties allows us to identify the volcanic potential of Jeju island. The low heat flow on Jeju island suggests that the volcano of Halla mountain may not be active. The high *Lg Q*, high V_P/V_S ratios and high crustal *P* amplification around Jeju island suggests the presence of solidified mafic body in the crust and volcanic sediments and lava on the surface.

The general anti-correlations between *Lg Q* and crustal *P* amplification and between the V_P/V_S ratios and *Pn* velocities and the positive correlations between the upper-crustal *S* velocities and *Lg Q* (or crustal *P* amplification) in most regions except the Gyeongsang basin suggest a general consistency in structures between the upper and lower crusts. This observation suggests that the tectonic structures observed on the Earth's surface, with the exception of the Gyeongsang basin, generally extend to the mantle lid.

10. Conclusions

The Korean Peninsula is located in the eastern margin of the Eurasian plate, and has experienced complex tectonic evolution. The properties of the crust allow us to understand past tectonic activities and potential seismic hazards. In this study, we investigated the V_P/V_S ratios in the upper crust of the Korean Peninsula using local *P* and *S* travel times and a modified Wadati analysis.

The V_P/V_S ratios were determined to be 1.60–1.91, with an average of 1.69. The corresponding Poisson's ratios are 0.18–0.32 with an average of 0.23. The V_P/V_S ratios are as high as 1.73–1.91 in the volcanic or basaltic regions, and are as low as 1.64–1.72 in the massif regions. High V_P/V_S ratios are observed in the Yeonil and eastern Gyeongsang basins, the offshore region of the eastern Okcheon belt, the south-central Gyeonggi massif and Jeju island.

The stability of the results was tested for plausible errors in the data and analysis. The possible V_P/V_S variations for inclusion of errors in travel-time data are small enough to support the results observed in this study. In addition, the stability test, which is based on a bootstrapping method, presented nearly constant V_P/V_S ratios throughout the upper crust, excluding the topmost sedimentary layers on the surface, which typically exhibit high V_P/V_S ratios (e.g., Nicholson and Simpson, 1985).

The V_P/V_S ratios were compared with composite sets of seismic and geophysical properties including heat flows, gravity anomalies, upper-crustal shear-wave velocities, Moho *P*-wave (*Pn*) velocities, crustal *P*-wave amplification factors, crustal-guided shear-wave attenuation factors (*Lg Q*), and surface topography. The V_P/V_S ratios are correlated well with the geophysical and seismic properties. This combined analysis of various seismic and geophysical quantities helps us understand the properties and characteristics of the crust in the Korean Peninsula.

Strong negative correlations were observed between the heat flows and *Pn* velocities. We found relatively low V_P/V_S ratios in the regions with low heat flows. The crustal shear-wave velocities were found to be high in regions with low V_P/V_S ratios and heat flows. The lateral variations in Bouguer gravity anomalies are similar to those of upper-crustal *S*-wave velocities and crustally-guided shear-wave attenuation. In addition, the *P* amplification rates are compatible with the crustally-guided shear-wave attenuation (*Lg Q*). The similarity between the *P* amplification rates and *Lg Q* suggests a correlation between the *P* and *S* wave structures.

The Gyeongsang basin is a Cretaceous sedimentary layer over the Yeongnam massif. The presence of the sedimentary layer is clearly identified by various geophysical and seismic properties of the upper crust, including the shear-wave velocities, Bouguer gravity anomalies, and the *P* amplification rates. The general correlations among various geophysical and seismic properties in most regions, except the Gyeongsang basin, also suggest that the geological provinces observed on the Earth's surface may extend to the lithospheric mantle.

Acknowledgements

We thank Dr. Xiaobo He for an early version of the travel time data of local *P* and *S* waves, and Dr. Youngmin Lee for heat flow data of the southern Korean Peninsula. We are grateful to the Korea Meteorological Administration (KMA) and the Korea Institute of Geoscience and Mineral Resources (KIGAM) for making seismic data available. We also thank Professors Moonsup Cho and Dapeng Zhao (editor) for careful review of the paper. This work was supported by the Korea Meteorological Administration Research and Development Program under Grant CATER 2012-8050.

References

Birch, F., 1961. The velocity of compressional waves in rocks to 10 kilobars, Part 2. Journal of Geophysical Research 66, 2199–2224.
Black, P.R., Braile, L.W., 1982. Pn velocity and cooling of the continental lithosphere. Journal of Geophysical Research 87, 10,557–10,568.
Carpenter, P.J., Cash, D.J., 1988. Poisson's ratio in the Valles caldera and Rio Grande rift of northern New Mexico. Bulletin of the Seismological Society of America 78, 1826–1829.
Chang, S.J., Baag, C.E., 2005. Crustal structure in southern Korea from joint analysis of teleseismic receiver functions and surface-wave dispersion. Bulletin of the Seismological Society of America 95, 1516–1534.
Chang, S.J., Baag, C.E., 2007. Moho depth and crustal V_P/V_S variation on southern Korea from teleseismic receiver functions: implication for tectonic affinity between the Korean Peninsula and China. Bulletin of the Seismological Society of America 97, 1621–1631.
Chatterjee, S.N., Pitt, A.M., Iyer, H.M., 1985. V_p/V_s ratios in the Yellowstone National Park region, Wyoming. Journal of Volcanology and Geothermal Research 26, 213–230.
Chiarabba, C., Amato, A., 2003. V_p and V_p/V_s images in the Mw 6.0 Colfiorito fault region (central Italy): a contribution to the understanding of seismotectonic and seismogenic processes. Journal of Geophysical Research 108 (B5), 2248. http://dx.doi.org/10.1029/2001JB001665.
Cho, M., Kim, H., 2005. Metamorphic evolution of the Ogcheon belt, Korea: a review and new age constraints. International Geology Review 47, 41–57.
Cho, J.-D., Choi, J.-H. Lim, M.-T. Park, I.-H. and Ko, I.-S., 1997. A Study on the Regionl Gravity Anomaly (Southern Part of Korean Peninsula), KIGAM Research Report KR-96(c)-5, Korea Institute of Geology and Mining and Materials, p. 27 (in Korean).
Cho, H.M., Kim, H.J., Jou, H.T., Hong, J.-K., Baag, C.-E., 2004. Transition from rifted continental to oceanic crust at the southeastern Korean margin in the East Sea (Japan Sea). Geophysical Research Letters 31, L07606, 1029/2003Gl019107.
Cho, H.M., Baag, C.-E., Lee, J.M., Moon, W.M., Jung, H., Kim, K.Y., Asudeh, I., 2006. Crustal velocity structure across the southern Korean Peninsula from seismic refraction survey. Geophysical Research Letters 33, L06307. http://dx.doi.org/10.1029/2005GL025145.
Choi, H.I., 1986. Sedimentation and evolution of the Cretaceous Gyeongsang Basin, southeastern Korea. Journal of the Geological Society 143, 29–40.
Choi, J., Kang, T.-S., Baag, C.-E., 2009. Three-dimensional surface wave tomography for the upper crustal velocity structure of southern Korea using seismic noise correlations. Geosciences Journal 13 (4), 423–432.
Choi, H., Hong, T.-K., He, X., Baag, C.-E., 2012. Seismic evidence for reverse activation of a paleo-rifting system in the East Sea (Sea of Japan). Tectonophysics, 123–133.
Chough, S.K., Kwon, S.-T., Ree, J.-H., Choi, D.-K., 2000. Tectonic and sedimentary evolution of the Korean Peninsula: a review and new view. Earth Science Reviews 52, 175–235.
Chough, S.K., Kim, H., Woo, J., Lee, H.S., 2006. Tectonic implications of quartzite-shale and phyllite beds in the Seochangri Formation (Okcheon Group), Bonghwajae section, mid-Korea. Geosciences Journal 10 (4), 403–421.
Christensen, N.I., 1996. Poisson's ratio and crustal seismology. Journal of Geophysical Research 101, 3139–3156.
Eberhart-Phillips, D., Reyners, M., Chadwick, M., Chiu, J.-M., 2005. Crustal heterogeneity and subduction processes: 3-D V_p, V_p/V_s and Q in the southern North Island, New Zealand. Geophysical Journal International 162, 270–288.
Efron, B., Tibshirani, R., 1991. Statistical data analysis in the computer age. Science 253, 390–395.
Fernández-Viejo, G.R.M., Clowes, Welford, J.K., 2005. Constraints on the composition of the crust and uppermost mantle in northwestern Canada: V_P/V_S variations along Lithoprobe's SNorCLE. Canadian Journal of Earth Sciences 42, 1205–1222.
Fitch, T.J., Rynn, J.M.W., 1976. Inversion for V_p/V_s in shallow source regions. Geophysical Journal of the Royal Astronomical Society 44 (1), 253–267.
Griggs, D.T., Jackson, D.D., Knopoff, L., Shreve, R.L., 1975. Earthquake prediction: modeling the anomalous V_p/V_s source region. Science 187, 537–539.
He, X., Hong, T.-K., 2010. Evidence for strong ground motion by waves refracted from the Conrad discontinuity. Bulletin of the Seismological Society of America 100 (3), 1370–1374.
Hong, T.-K., 2010. Lg attenuation in a region with both continental and oceanic environments. Bulletin of the Seismoligical Society of America 100, 851–858.
Hong, T.-K., Choi, H., 2012. Seismological constraints on the collision belt between the North and South China blocks in the Yellow Sea. Tectonophysics, 102–113.
Hong, T.-K., Kang, T.-S., 2009. Pn Travel-Time tomography of the paleo-continental-collision and rifting zone around Korea and Japan. Bulletin of the Seismoligical Society of America 99, 416–421.

Hong, T.-K., Lee, K., 2012. mb(Pn) scale for the Korean Peninsula and site-dependent Pn amplification. Pure and Applied Geophysics 169 (11), 1963–1975.

Hong, T.-K., Menke, W., 2008. Imaging laterally varying regional heterogeneities from seismic coda using a source-array analysis. Physics of the Earth and Planetary Interiors 166, 188–202.

Hong, T.-K., Kennett, B.L.N., Wu, R.-S., 2004. Effects of the density perturbation in scattering. Geophysical Research Letters 31 (13), L13602. http://dx.doi.org/10.1029/2004GL019933.

Hong, T.-K., Baag, C.-E., Choi, H., Sheen, D.-H., 2008. Regional seismic observations of the 9 October 2006 underground nuclear explosion in North Korea and the influence of crustal structure on regional phases. Journal of Geophysical Research 113, B03305. http://dx.doi.org/10.1029/2007JB004950.

Jaupart, C., Mareschal, J.-C., 2007. Heat flow and thermal structure of the lithospheres. In: Treatise on Geoophysics. Crust and Lithosphere Dynamics, vol. 6. Elsevier, Spain, pp. 217–251.

Ji, S., Wang, Q., Salisbury, M.H., 2009. Composition and tectonic evolution of the Chinese continental crust constrained by Poisson's ratio. Tectonophysics 463, 15–30.

Jiménez, M.J., García-Fernández, M., 1996. Aftershock sequence of the 9 May 1989 Canary Islands earthquake. Tectonophysics 255, 157–162.

Julian, B.R., Ross, A., Foulger, G.R., Evans, J.R., 1996. Three-dimensional seismic image of a geothermal reservoir: The Geysers, California. Geophysical Research Letters 23 (6), 685–688.

Lee, Y.M., Park, S., Kim, J., Kim, H.C., Koo, M.-H., 2010. Geothermal resource assessment in Korea. Renewable and Sustainable Energy Reviews 14, 2392–2400.

Lillie, R.J., 1998. Whole Earth Geophysics: An Introductory Textbook for Geologists and Geophysicists. Prentice Hall, Toronto, p. 361.

Lin, J.-Y., Sibuet, J.-C., Lee, C.-S., Hsu, S.-K., Klingelhoefer, F., 2007. Origin of the southern Okinawa Trough volcanism from detailed seismic tomography. Journal of Geophysical Research 112, B08308. http://dx.doi.org/10.1029/2006JB004703.

MacKenzie, L., Abers, G.A., Fischer, K.M., Syracuse, E.M., Protti, J.M., Gonzalez, V., Strauch, W., 2008. Crustal structure along the southern Central American volcanic front. Geochemistry Geophysics Geosystems 9 (8), Q08S09. http://dx.doi.org/10.1029/2008GC001991.

Mjelde, R., Aurvøag, R., Kodaira, S., Shimamura, H., Gunnarsson, K., Nakanishi, A., Shiobara, H., 2002. V_P/V_S-ratios from the central Kolbeinsey ridge to the Jan Mayen basin, north Atlantic; implications for lithology, porosity and present-day stress field. Marine Geophysical Researches 23, 125–145.

Moretti, M., De Gori, P., Chiarabba, C., 2009. Earthquake relocation and three-dimensional V_p and V_p/V_s models along the low angle Alto Tiberina Fault (Central Italy): evidence for fluid overpressure. Geophysical Journal International 176, 833–846.

Musacchio, G., Mooney, W.D., Luetgert, J.H., Christensen, N.I., 1997. Composition of the crust in the Grenville and Appalachian Provinces of North America inferred from V_P/V_S ratios. Journal of Geophysical Research 102 (B7), 15,225–15,241.

Nakajima, J., Matsuzawa, T., Zhao, D., 2001. Three-dimensional structure of V_p, V_s, and V_P/V_S beneath northeastern Japan: implications for arc magmatism and fluids. Journal of Geophysical Research 106, 21,843–21,857.

Nicholson, C., Simpson, D.W., 1985. Changes in V_P/V_S with depth: Implications for appropriate velocity models, improved earthquake locations, and material properties of the upper crust. Bulletin of the Seismological Society of America 75, 1105–1123.

Oh, C.W., 2006. A new concept on tectonic correlation between Korea, China and Japan: histories from the late Proterozoic to Cretaceous. Gondwana Research 9, 47–61.

Ojeda, A., Havskov, J., 2001. Crustal structure and local seismicity in Colombia. Journal of Seismology 5 (4), 575–593.

Revenaugh, J., Meyer, R., 1997. Seismic evidence of partial melt within a possibly ubiquitous low-velocity layer at the base of the mantle. Science 277, 670–673.

Reyners, M.D., Eberhart-Phillips, G., Stuart, Nishimura, Y., 2006. Imaging subduction from the trench to 300 km depth beneath the central North Island, New Zealand, with V_p and V_p/V_s. Geophysical Journal International 165, 565–583.

Rudnick, R.L., Fountain, D.M., 1995. Nature and composition of the continental crust: a lower crustal perspective. Review of Geophysics 33, 267–309.

Sagong, H., Kwon, S.-T., Ree, J.-H., 2005. Mesozoic episodic magmatism in South Korea and its tectonic implication. Tectonics 24, TC5002. http://dx.doi.org/10.1029/2004TC001720.

Salah, M.K., Seno, T., 2008. Imaging of V_p, V_s, and Posson's ratio anomalies beneath Kyushu, southwest Japan: implications for volcanism and forearc mantle wedge serpentinization. Journal of Asian Earth Sciences 31, 404–428.

Sandvol, E., Seber, D., Calvert, A., Barazangi, M., 1998. Grid search modeling of receiver functions: implications for crustal structure in the Middle East and North Africa. Journal of Geophysical Research 103, 26,899–26,917.

Sato, H., Fehler, M., 1998. Seismic Wave Propagation and Scattering in the Heterogeneous Earth. Springer-Verlag, New York.

Shapiro, N.M., Campillo, M., Stehly, L., Ritzwoller, M.H., 2005. High resolution surface wave tomography from ambient seismic noise. Science 307, 1615–1618.

Tatham, R., 1982. V_p/V_s and lithology. Geophysics 47 (3), 336–344.

Thurber, C.H., Atre, S.R., 1993. Three-dimensional V_p/V_s variations along the Loma Prieta rupture zone. Bulletin of the Seismological Society of America 83 (3), 717–736.

Tondi, R., Achauer, U., Landes, M., Daví, R., Besutiu, L., 2009. Unveiling seismic and density structure beneath the Vrancea seismogenic zone, Romania. Journal of Geophysical Research 114, B11307. http://dx.doi.org/10.1029/2008JB005992.

Wadati, K., 1933. On the travel time of earthquake waves, II. Geophysical Magazine 7, 101–111.

Whattam, S.A., Cho, M., Smith, I.E.M., 2011. Magmatic peridotites and pyroxenites, Andong Ultramafic Complex, Korea: geochemical evidence for supra-subduction zone formation and extensive melt–rock interaction. Lithos 127, 599–618.

Wu, Y.-M., Chang, C.-H., Zhao, L., Shyu, J.B.H., Chen, Y.-G., Sieh, K., Avouac, J.-P., 2007. Seismic tomography of Taiwan: improved constraints from a dense network of strong motion stations. Journal of Geophysical Research 112, B08312. http://dx.doi.org/10.1029/2007JB004983.

Yoshiyama, R., 1957. The ratio of the velocity of P and S waves. Bulletin of the Earthquake Research Institute, University of Tokyo 35 (4), 627–640.

Zhang, H., Thurber, C.H., Shelly, D., Ide, S., Beroza, G.C., Hasegawa, A., 2004. High-resolution subducting-slab structure beneath northern Honshu, Japan, revealed by double-difference tomography. Geology 32 (4), 361–364.

Zhao, D., Mishra, O.P., Sanda, R., 2002. Influence of fluids and magma on earthquakes: seismological evidence. Physics of the Earth and Planetary Interiors 132, 249–267.

Zhu, L., Kanamori, H., 2000. Moho depth variation in southern California from teleseismic receiver function. Journal of Geophysical Research 105, 2969–2980.